REVIEW ARTICLE

DᵛSᴇ WILEY

Seabed structures and foundations related to deep-sea resource development: A review based on design and research

Shengjie Rui[1,2] | Haojie Zhang[1] | Hang Xu[1] | Xing Zha[1] | Mengtao Xu[1] | Kanmin Shen[3]

[1]Key Laboratory of Offshore Geotechnics and Material of Zhejiang Province, College of Civil Engineering and Architecture, Zhejiang University, Hangzhou, China

[2]Advanced Modelling, Offshore Energy, Norwegian Geotechnical Institute, Oslo, Norway

[3]Geotechnical Technology Center (Overseas Engineering Center), PowerChina Huadong Engineering Corporation Limited, Hangzhou, China

Correspondence
Kanmin Shen, Geotechnical Technology Center (Overseas Engineering Center), PowerChina Huadong Engineering Corporation Limited, Hangzhou 311122, China.
Email: shenkanmin@163.com

Abstract

The deep-sea ground contains a huge amount of energy and mineral resources, for example, oil, gas, and minerals. Various infrastructures such as floating structures, seabed structures, and foundations have been developed to exploit these resources. The seabed structures and foundations can be mainly classified into three types: subsea production structures, offshore pipelines, and anchors. This study reviewed the development, installation, and operation of these infrastructures, including their structures, design, installation, marine environment loads, and applications. On this basis, the research gaps and further research directions were explored through this literature review. First, different floating structures were briefly analyzed and reviewed to introduce the design requirements of the seabed structures and foundations. Second, the subsea production structures, including subsea manifolds and their foundations, were reviewed and discussed. Third, the basic characteristics and design methods of deep-sea pipelines, including subsea pipelines and risers, were analyzed and reviewed. Finally, the installation and bearing capacity of deep-sea subsea anchors and seabed trench influence on the anchor were reviewed. Through the review, it was found that marine environment conditions are the key inputs for any offshore structure design. The fabrication, installation, and operation of infrastructures should carefully consider the marine loads and geological conditions. Different structures have their own mechanical problems. The fatigue and stability of pipelines mainly depend on the soil-structure interaction. Anchor selection should consider soil types and possible trench formation. These focuses and research gaps can provide a helpful guide on further research, installation, and operation of deep-sea structures and foundations.

KEYWORDS
anchors, floating structures, pipelines, risers, subsea foundations

Highlights
- Provide a brief introduction about seabed structures and foundations related to deep-sea resource development.
- Introduce subsea production structures, including subsea manifolds and their foundations (mudmats, suction piles), from a design perspective.
- Analyze the basic characteristics and design methods of deep-sea pipelines, including subsea pipelines and risers.
- Introduce the installation and bearing capacity of anchors in deep-sea, and summarize seabed trench influence on anchor capacity.

1 | INTRODUCTION

Oil & gas exploitation originated in offshore regions since 1897. Wells at sea at first manufactured oil in California (Hyne, 2001). Production has since moved towards deeper marine areas since the 1960s due to the depletion of easily accessible resources. With improved technology for production, large reserves of oil and gas were exploited (Cordes et al., 2016). At present, the oil & gas exploitation is common in various marine environments. The major deep-sea areas include the Gulf of Mexico, Africa coastal region, northern North Sea, Australia, and Southeast Asia. Ultra-deep-water production of more than 1500 m develops rapidly in the Gulf of Mexico and West Africa, where the depth can reach 2000 m (Murawski et al., 2020).

In fact, the deep-sea oil & gas exploration contains multiple steps. The first step is to detect potential hydrocarbon reservoirs based on acoustic remote sensing (Gausland, 2003; Kark et al., 2015). After detection, some exploration wells are drilled to validate the detected data and locate the reservoirs (Sahu et al., 2020). After the economic and feasibility assessment of hydrocarbon reserves are verified, the production on the site may proceed (Hyne, 2001). The oil & gas exploration typically contains some equipment, for example, the device for well drilling, the floating structures, and subsea infrastructure (Bai & Bai, 2018). For example, the water depths of the BP Greater Plutonio field off Angola are between 1200 and 1500 m, and the area is about 140 km^2. During the operational period, the oil and gas is transported through tankers and pipelines (Boesch & Rabalais, 1987).

The oil & gas exploitations accelerate the rapid development of deep-sea structures, including floating structures, subsea structures, and foundations. Some structures at the seabed are located in the deep-sea region, which are vital for the oil & gas exploitation. If these seabed structures are damaged or failed, it is very difficult to repair these structures, thus inducing heavy losses. For the further development of these seabed structures and foundations, this paper reviews the seabed structures and foundations related to deep-sea resource development.

The structure of this paper is as follows. First, different floating structures were briefly analyzed and reviewed, which provided the overall background for seabed structures. Then, the subsea production structures, including subsea manifolds and their foundations (mudmats, suction piles), were reviewed and discussed. Third, the basic characteristics and design methods of deep-sea pipelines, including subsea pipelines and risers, were analyzed and reviewed. Finally, the installation and bearing capacity of deep-sea subsea anchors were analyzed, and the influence of seabed trench on the anchor was explored.

2 | FLOATING STRUCTURES

In this section, floating structures and marine environment loads are briefly introduced to provide the overall background for Sections 3–5.

2.1 | Deep-sea floating structures

Different types of the floaters have been developed for the oil & gas exploitation in the deep-sea to produce resources (Ma et al., 2019). As shown in Figure 1, the floating structures widely used include the semi-submersible platform, tension leg platform (TLP), Spar platform, and floating production storage offloading (FPSO).

2.1.1 | Semi-submersible platform

Semi-submersible platforms include several columns and pontoons to reduce the water surface line and wave loads (Gonçalves et al., 2013). Semi-submersibles are popular in the deep-sea region due to their spacious deck and easy installation (Ma et al., 2019). Recently, a series of typical semi-submersible platforms for the oil & gas
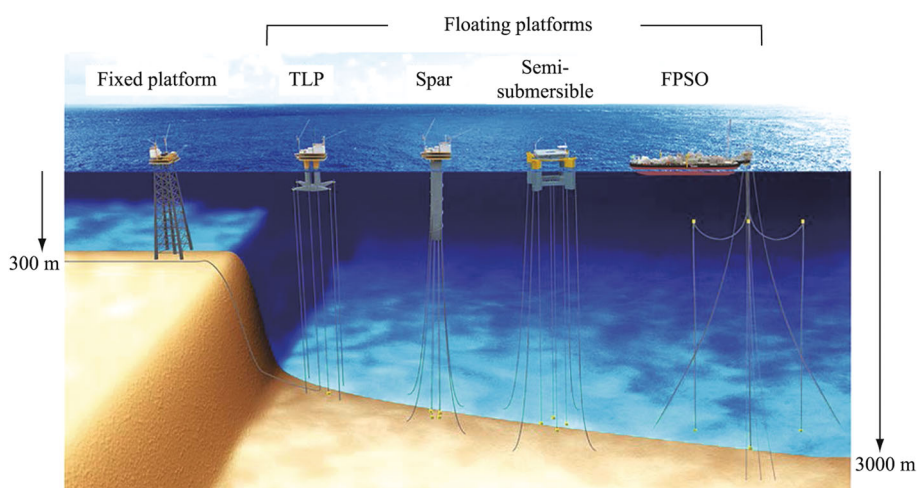

FIGURE 1 Deepwater floating platform types. FPSO, floating production storage offloading; TLP, tension leg platform.

exploitation, for example, Hai Yang Shi You 981 platform with 4 × 3 symmetrical layout of mooring lines, Deep-sea No. 1 platform with four columns and four pontoons, have been constructed and put into operation successfully.

2.1.2 | TLP

The TLP is a kind of floating platform which is vertically moored through mooring lines/tendons at the platform corner (Bachynski & Moan, 2012). The platform is suitable for water depths of 300–1500 m (Figure 1). The tendons/mooring lines have relatively large axial stiffness, so that the platform has less vertical motion (Niedzwecki & Huston, 1992). Under these conditions, the production wellheads can be fixed on the platform deck and connected to the wells at the seabed via risers.

2.1.3 | Spar platform

Spar platform refers to a kind of platform commonly adopted in the deep-sea region (Figure 1). A Spar is made up of a cylinder with a large diameter which is adopted to hold a high deck (Agarwal & Jain, 2003). The bottom of cylinder is covered with a special material with high density to reduce the height of the gravity center and improve its stability. In addition, the cylinder is encircled by strakes to reduce motions caused by vortex-induced vibration (Ma et al., 2019). Spars are positioned by spread mooring systems composed of multicomponents.

2.1.4 | FPSO

FPSO, which is a ship-shaped vessel adopted in the oil and gas manufacture (Duggal & Minnebo, 2020). An FPSO is designed to store oil and gas from seabed wells or equipment until the hydrocarbons/oil can be transported through a pipeline or offloaded by a shuttle tanker. Thus, FPSOs are usually the preferred platform in these regions without local pipelines to export oil. A mooring system with multi-mooring lines can be adopted to keep the position for FPSOs (Rho et al., 2013).

2.2 | Marine environment loads

The deep-sea marine environment loads are the main input parameters for the design of floaters and their subsidiary structures. Figure 2 presents the main loads, including wind, wave, current, and ice. The load magnitude and direction affect the application of floaters and their subsidiary structures (Ma et al., 2019). In the following parts, the main marine environment loads will be briefly introduced.

2.2.1 | Wind loads

Wind mainly contributes to the static load and low-frequency load acting on the offshore structures (Zhou et al., 2019). Wind is also one resource of the waves and current, which is usually described by the magnitude and direction, and the actual engineering depends on the wind spectrum. The wind spectrum is an expression of the dynamic properties of the wind (turbulence), which reflects the fluctuations in the same direction as a certain mean wind speed. The wind speed changes depending on the position and time (Figure 2), and the speed is lower near the sea surface than that far away from the sea level (Ma et al., 2019). Therefore, the wind speed refers to the average value during a specific time, for example, 10 min, at a reference height, for example, 10 m. Wind direction usually refers to the direction from which the wind generates. The wind velocity changes with position. Different models of wind profiles can be adopted depending on the offshore industries, for example, bottom-fixed offshore wind turbines (Wang, Zhou, et al., 2020; Zha et al., 2022; Zhou, Guo, Wang, Li, Li, et al., 2021).

2.2.2 | Wave loads

Waves can be divided into swell and wind waves according to their origins. Wind waves are generated
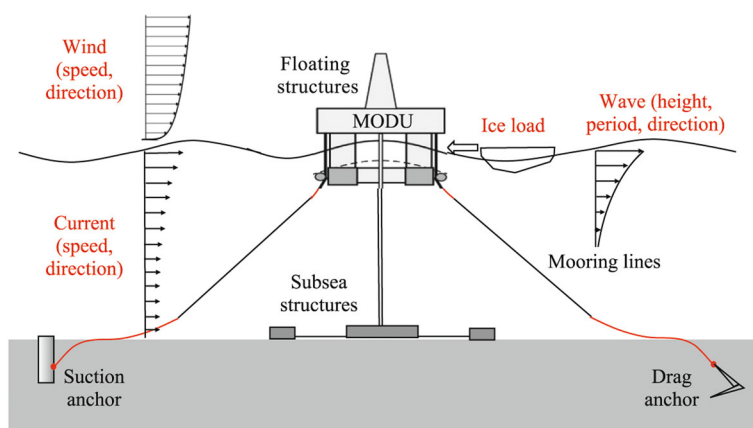
FIGURE 2 Deep-sea environment loads on floating structures. MODU, name of a platform.

from the local wind (Young, 1999) and propagate to other places. A swell refers to the wave generated from global regions where wind blasts for a long period above the sea. Wave height is the vertical distance between the crest (peak) and the trough of a wave. The wavelength of a swell is not apparently influenced by the local wind. A swell also has a long wave period, and can be roughly described by the Gaussian spectrum with a narrow band. Wave direction commonly refers to the direction from which the waves are generated.

2.2.3 | Current loads

Current refers to the relatively stable flow of the seawater in a large range. The direction of current refers to the orientation which the current flows to. The current profile describes the speed at different positions of the sea. In general, the current is considered a steady load, which generates drag and lift forces. The current velocity changes with the water depth. The current loads on the floaters are described by force coefficients, which is similar to wind. The current usually increases the forces on the structures but may counterbalance loads depending on its direction.

2.3 | Brief summary

The floating structures mainly consist of four types, which adapt to the different environment conditions and design requirements. Spar platforms adapt to relatively deep water, and TLP platforms need larger mooring line tension. Semi-submersible platforms are easier to be installed, and FPSOs are the most flexible ones in practice. The accurate calculation of environment loads, including wind, wave, current, is necessary for offshore structure design.

3 | SUBSEA PRODUCTION STRUCTURES

In this section, the subsea production structures are introduced, including subsea manifolds and their main foundations (e.g., mudmat, suction pile). The design and installation of subsea manifolds are mainly introduced from the perspective of structural mechanics. The foundations, for example, mudmats and suction piles, are analyzed mainly from the soil-structure interaction.

3.1 | Subsea manifold

Subsea manifolds are designed to optimize pipelines and risers to promote efficiency. Figure 3 presents a sketch of manifold and its surrounding structures, with pipelines and valves to combine and distribute fluid flow (Rose, 2008). Different types of manifolds have been developed, for example, a simple pipeline end manifold (PLEM) and a subsea process system.
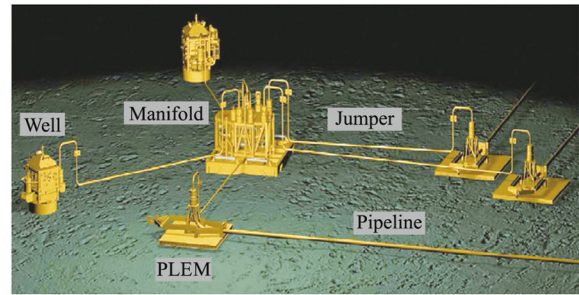

FIGURE 3 Subsea manifold and its connected structures (Rose, 2008).

A manifold system usually consists of a manifold, a foundation, and a supporting structure. A supporting structure provides facilities to match the manifold with the foundation in the seabed. A manifold is a steel frame equipped with pipes, valves, flow meters, control module, and so forth. A foundation is a structure interacting with seabed to support the manifold. It can be a suction pile or a mudmat, depending on soil properties and manifold dimensions.

3.1.1 | PLEM

A PLEM is a kind of simple manifold, which connects a pipeline to other subsea structures through a jumper, as shown in Figure 4. A PLEM generally consists of: (1) piping components; (2) a structural frame supporting the components; (3) a foundation providing the seabed resistance; (4) installation yokes connected to the frame.

3.1.2 | Design and analysis

The design procedure for the PLEM follows four steps: (1) architecture design considering the geometry, installation, and fabrication; (2) determining initial sizes, including the load path, the primary components; (3) modeling the structures for analysis, including the finite element (FE) three-dimensional model; (4) stress analysis to satisfy the design criteria.

Structural design and analysis
The design of a PLEM should be conducted based on SACS/StruCAD in accordance with API-RP-2A-WSD (2006). The PLEM analysis should consider the conditions of in-place operating condition, installation, transportation, fabrication, and so forth.

Mudmat design and analysis
A mudmat dimension of a PLEM is evaluated according to the soil resistance and the structure weights. The strength profiles of the soil are acquired through site investigation of seabed. The averaged value at a certain depth is the designed shear strength. The foundation holding capacities are evaluated in the installation and operation conditions.

A mudmat should be designed according to API-RP-2A-WSD (2020) or DNV (1992). The design should
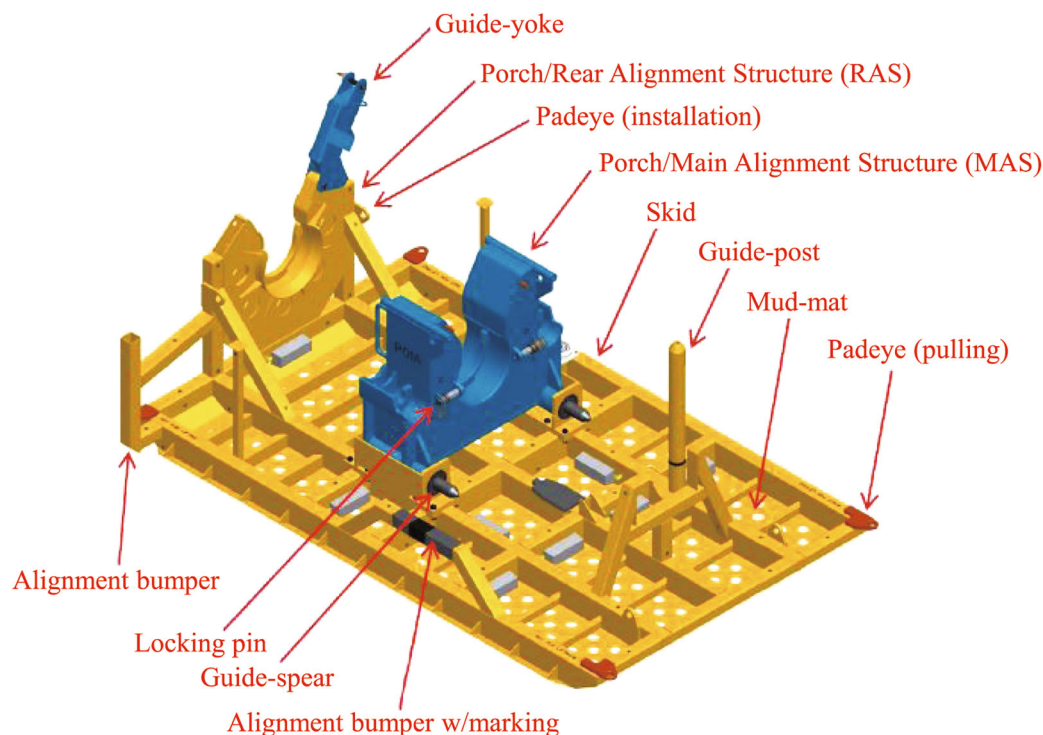
FIGURE 4 Sketch of a pipeline end manifold (PLEM) (nfatmala.blogspot.com/2016/02/pipeline-ending-manifold-plemplet.html).

consider the eccentric loading, overturning, settlement, sliding, torsional failures, and cyclic effects. Mudmats equipped with embedded skirts are manufactured to maintain the stability and to decrease their movement and settlement in clay. However, PLEMs without skirts are often adopted in sand seabed, so they can move freely due to the small penetration.

3.1.3 | PLEM installation analysis

During installation and operation, the PLEM needs to be steady on the seabed with the correct direction. The first-end PLEM is adopted to start pipelay, and a second-end PLEM is finally installed after the pipelay is finished. The problems that should be considered during installation include: too high center of gravity, redundant measures to land vertically, and pipe breakage because of large settlement. S-lay or J-lay can be selected in the installation of pipelines (discussed in Section 4).

The installation analysis for PLEM should check shear, bending, hoop stresses, and pipeline tension. The installation process consists of the following four steps: (1) installation of first-end PLEM; (2) normal pipeline installation; (3) abandonment of second-end PLEM; (4) recovery and abandonment. To ensure the pipeline integrity, the following evaluations should be carried out: (1) static analysis to determine the requirements, (2) wave analysis to determine the key environment cases, and (3) local buckling check.

3.2 | Mudmat

Foundations provide a supporting structure for the PLEM. As shown in Figure 5, the foundations can be divided into
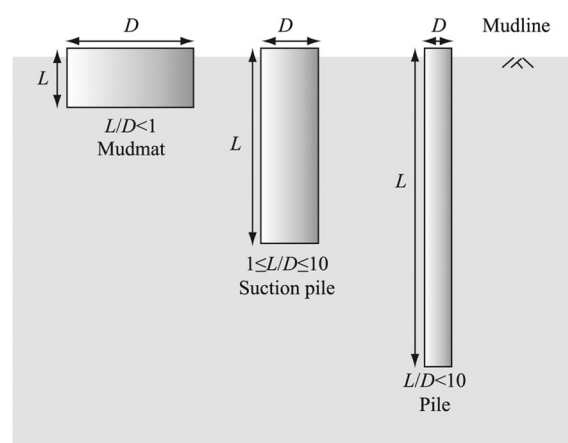

FIGURE 5 Foundations for subsea manifold and their size definitions.

three groups: (1) mudmat with $L/D < 1$; (2) suction pile with $1 \leq L/D \leq 10$; (3) pile with $L/D < 10$ (where L is the foundation length, and D is the foundation diameter) (Liu, Pisanò, et al., 2022; Liu, Sivasithamparam, et al., 2022). A preliminary mudmat dimensions are evaluated on the base of the soil properties and all component weights. The dimensions will be adjusted on the installation facilities, sea situations, fabrication shop, and so forth.

3.2.1 | Designed contents

The foundations supporting the PLEMs should satisfy the design criteria of API-RP-2A-WSD (2020), and the maximum factor of safety is 2.0. The design should consider the following items: (1) stability to avoid failure because of bearing, overturning, sliding, and combined loads; (2) large

deformation and damage of the structure components; (3) dynamic characteristics of structural response under dynamic loads; (4) hydraulic stability, for example, local scour owing to currents; (5) installation and removal.

3.2.2 | Geotechnical design

Overturning capacity

The overturning capacity calculation is to ensure the stability of the foundation on the seabed under the applied loads. Overturning could appear in both longitudinal and transverse directions. The governing overturning condition meets the minimum factor of safety, which can be calculated by

$$FS_{o-t} = \frac{F_z L_d}{M},\tag{1}$$

where M denotes the resultant overturning moment (kN m); F_z is the vertical component of resultant force (kN); and L_d represents the distance from its geometric center to rotating axis (m). The ultimate vertical load for a foundation is reduced by load eccentricity, which can be considered by decreasing the footing area.

Penetration resistance of skirts

Skirts are designed to ensure that the structures maintain their stability with the maximum consolidation settlement. The penetration resistance of skirt in sand can be calculated by (Andersen & Jostad, 1999)

$$Q_P = q_t A_t + \tau_w A_w,\tag{2}$$

where q_t is skirt tip pressure, $q_t = k_p q_{c,CPT}$; τ_w denotes skirt wall friction, $\tau_w = k_f q_{c,CPT}$; k_p and k_f are the correction factors of tip resistance and wall friction, respectively; A_t represents skirt tip area, and A_w skirt surface area; $q_{c,CPT}$ refers to the resistance evaluated based on CPT test.

Bearing capacity during installation

The minimum dimensions of mudmats change with the soil vertical capacity considering the resultant load eccentricities. For the sand seabed, the vertical holding capacity can be calculated by

$$Q_v = 0.5 N_\gamma \gamma' B A + N_q p' A,\tag{3}$$

where N_γ, N_q are the bearing capacity factors; γ' is the sand effective unit weight; B is mudmat width; and p' is the effective vertical stress. For clay, the vertical capacity can be calculated by

$$Q_v = N_c S_u A,\tag{4}$$

where N_c is the load factor; S_u is the average undrained shear strength; A is the area of mudmat foundation.

Bearing capacity during operation

For the horizontal sliding, the soil resistance due to lateral sliding failure mechanism can be calculated by

$$Q_h = r \times \tan \varphi \cdot W,\tag{5}$$

where $r \times \tan \varphi$ is the foundation-seabed friction and W is the vertical component of loads acting on the mudmat. If a rock berm is placed on the mudmat, the lateral resistance can be acquired by

$$Q_v = P_p - P_a = (k_p + k_a)^{0.5} \gamma' H_r B,\tag{6}$$

where k_p, k_a are the earth pressure coefficients; γ' is the rock unit weight; H_r is the rock height; B is the mudmat foundation width.

3.3 | Suction pile

The aspect ratio of the suction pile changes from 7:1 for soft clay to 2:1 for stiff clay based on the seabed conditions (Eltaher et al., 2003). Suctions was first applied in 1980s, and has a wide application in deep-sea due to its low cost and easy installation. Suction piles are usually adopted as the foundation for the following merits: fixed location on the seabed, simple installation procedures, no special shortcoming due to the water depth, and precisely defined bearing capacity (Colliat, 2002).

3.3.1 | Design methodology and loads

API-RP-2A-WSD (2020) provides guidelines to ensure the adequate foundation safety of suction piles. In the preliminary design, the L/D versus its weight can be optimized to meet the requirement that suction pressure are suitable for the seabed soil. The suction pile design should abide by API-RP-2A-WSD (2020).

The design loads of suction anchor should include: (1) the permanent loads including the dead load and long-term static load; (2) the live and dynamic loads changing in magnitude, direction, and position; (3) the environment loads, for example, current and wave loads; (4) the accidental loads, for example, fishing gear snagging.

3.3.2 | Geotechnical design and stability

The suction piles supporting the manifolds should have enough capacities to resist all loads from the manifold system, for example, compression, lateral, moment, and torsion. The safety of factor (FOS) is selected according to API-RP-2A-WSD (2020). Stability evaluations are conducted in two conditions of the vertical load and the horizontal load according to API-RP-2A-WSD (2020).

3.3.3 | Penetration analysis

Penetration analyzes of suction piles include the skirt resistance, under-pressure to reach the set depth, allowable under-pressure, and soil heave in the caisson (Figure 6). The penetration evaluation is usually carried

out based on the principles proposed by Andersen and Jostad (1999). Such evaluation includes penetration resistance, anchor self-weight, required under-pressure, allowable under-pressure, soil heave, and maximum penetration depth (Xu et al., 2023). The penetration resistance R_{TOT} is evaluated by

$$R_{TOT} = R_{side} + R_{tip}, \tag{7}$$

where R_{side} is the resistance along the wall sides due to the side shear, and R_{tip} is the bearing capacity at the skirt tip. The required under-pressure to penetrate the suction pile can be assessed by

$$\Delta u = (R_{TOT} - W')/A_{in}, \tag{8}$$

where W' is the submerged weight and A_{in} is the inside pile area. The allowable under-pressure with respect to
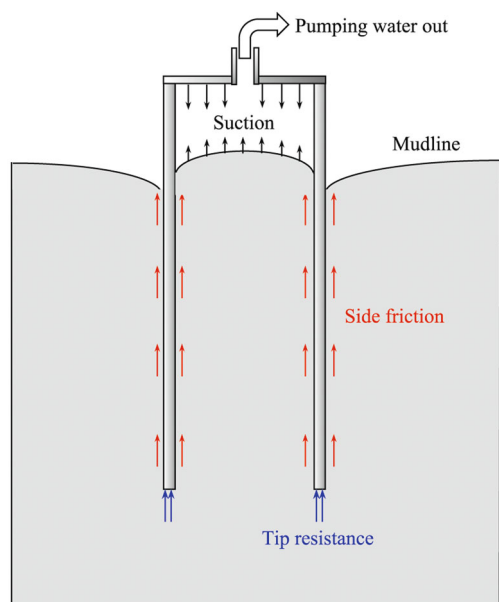
large soil heave due to bottom heave at the skirt tip level can be calculated by the bearing capacity. The required suction should be less than the allowable suction (Guo et al., 2012). Based on the assumption that the external (f_{out}) and the internal (f_{in}) frictions are equal, the resistance along the wall sides (R_{side}) can be calculated by

$$f_{out} = f_{in} = \alpha S_{u,DSS}, \tag{9}$$

where α is the adhesion factor; and $S_{u,DSS}$ refers to the average DSS shear strength. The installation with inside stiffeners in clays proves that the above method overestimates penetration force, which is because a mixture of remolded soil and water is captured by the stiffener, leading to low installation resistance. In this case, several analyzes are needed to address the friction generated on the inner skirt wall, which is related to the interface friction coefficient (Rui, Wang, Guo, Cheng, et al., 2021; Rui, Wang, Guo, Zhou, et al., 2021; Zhou et al., 2020; Zhou, Guo, Wang, Li, & Rui, 2021).

3.4 | Brief summary

The design of the PLEM should consider its fabrication and installation. The stress analyzes conducted by the FE models are also needed to satisfy the design criteria. The mudmat or suction pile should be selected and designed according to the soil properties and all component weights. For the mudmat, the overturning capacity and bearing capacity in the installation and operation should be analyzed. For the suction pile, the penetration forces of suction piles should be carefully assessed in particular.

4 | DEEP-SEA PIPELINES

The section introduces the slender deep-sea pipelines, which are used to transport hydrocarbon resources, as shown in Figure 7. The subsea flowlines refer to the pipelines transporting oil and gas from the seabed wells
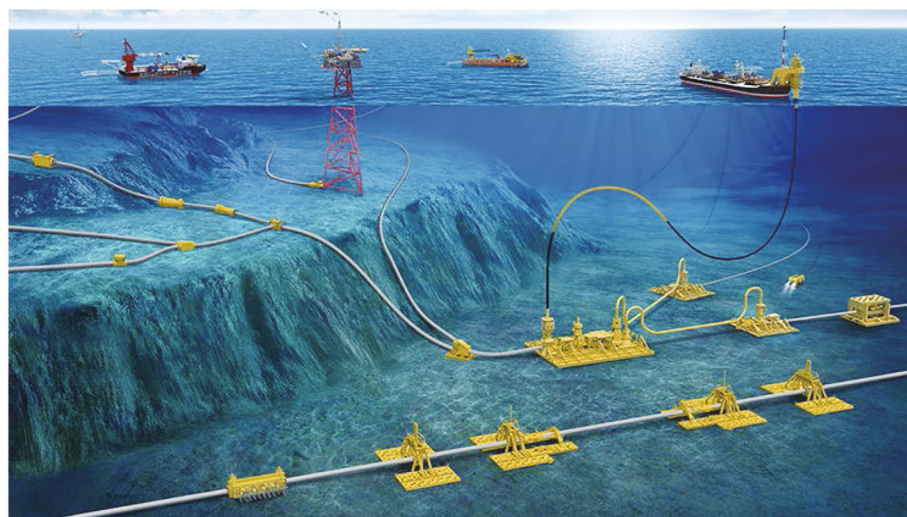

FIGURE 6 Force analysis of suction pile during installation.

FIGURE 7 Deep-sea pipelines (oilstates.com/offshore/subsea-pipeline-products/).
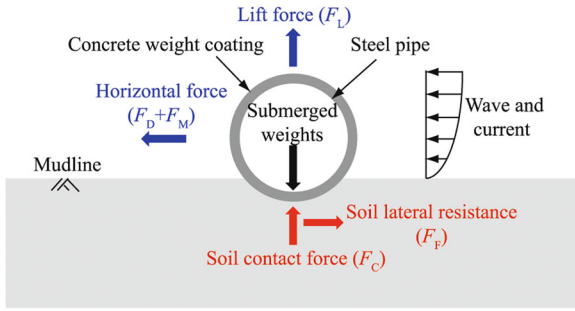
FIGURE 8 Forces acting on the subsea pipeline.

FIGURE 9 Generation of vortices in wake near spanning pipeline (Morse et al., 2017).

to the risers. The risers are pipelines connecting the subsea structures to the production facilities.

4.1 | Subsea pipelines

4.1.1 | On-bottom stability analysis

Subsea pipelines bear fluid loads induced by currents and waves (Yang, Guo, Wang & Qi, 2022; Yang, Guo, Wang, Dou, et al., 2022). For the seabed where the pipeline movement leads to its damage, it is required that the pipeline weight should be large enough to maintain its stability under the extreme conditions. In general, weight is added by placing a concrete coating around the pipeline (Guo, Stoesser, et al., 2022; Hafez et al., 2022).

The on-bottom stability is analyzed by the force equilibrium or FE analysis, as shown in Figure 8. The forces on the pipeline as the result of wave and current loads include the drag, lift, and inertia forces. The friction with the seabed caused by pipeline weight must balance these forces to ensure stability. The hydraulic forces are derived based on fluid mechanics by adopting suitable drag and lift coefficients depending on the pipeline dimensions and environmental loads (Yuan, Wang, Guo & Shi, 2012; Yuan, Wang, Guo & Xie, 2012). The effective flow contains two parts: (1) the steady current evaluated by boundary layer theory and (2) the wave-induced flow assessed by a suitable wave theory.

The wave and current data should adopt the data in extreme conditions. The friction with the seabed is dependent on soil properties and pipe weight, and provides resistance to maintaining the equilibrium of the pipelines. The fluid lift force counterbalances its weight. The lateral friction coefficient varies from 0.1 to 1.0 depending on the pipeline surface roughness and the soil. Soft clays and silts provide the least friction compared with coarse sands.

Figure 8 illustrates the forces for on-bottom stability analysis, meeting the following relationship:

$$\gamma(\boldsymbol{F_D} - \boldsymbol{F_I}) \le \mu(\boldsymbol{W_{sub}} - \boldsymbol{F_L}), \qquad (10)$$

where γ denotes the factor of safety (normally > 1.1); $\boldsymbol{F_D}$ is the unit drag force; $\boldsymbol{F_I}$ is the unit hydrodynamic inertia force; μ is the lateral soil friction coefficient; $\boldsymbol{W_{sub}}$ is the
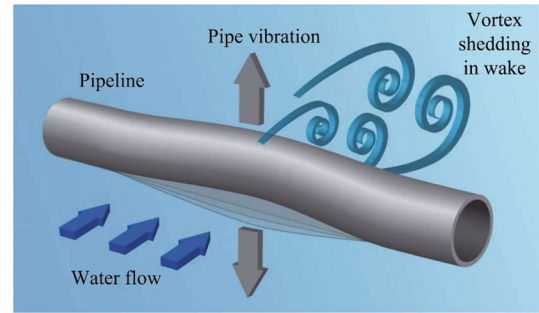
unit submerged pipe weight; and $\boldsymbol{F_L}$ refers to the unit lift force (the bold represents the vector).

The stability design relies on the empirical factors such as the force coefficients and soil friction factors. The value selection is closely related to the engineer experience and the specific design conditions. The purpose of stability evaluation is to acquire how much weight should be added by means of the coating.

4.1.2 | Free-span analysis

Over a rough seabed subjected to the scour, the pipeline spanning appears when the pipeline loses its contact with the seabed for a certain distance (Figure 9). Under these circumstances, design codes require that the pipeline design should consider yielding caused by loads, fatigue induced by vortex-induced vibration (VIV) and interference by human activities. These considerations raise a need for the assessment of suitable free-span length. If span length is larger than the allowable one, some measures are to be taken to shorten the span, thus inducing high costs. Consequently, span length assessment should be conducted as accurately as possible.

As shown in Figure 9, the wave and current flow near a pipeline span will lead to the vortices in wake (Guo et al., 2019). These vortices are shed from the pipe top and bottom, exerting oscillatory forces on the spanning pipelines. Vortex shedding indicates that currents would bring alternating loads on pipelines, resulting in pipe vibration. If the shedding frequency approaches the natural frequency, severe resonance would occur, thus inducing the pipe fatigue failure. Comparing the shedding frequency and the natural frequency is the method widely employed to evaluate the span so as to avoid the resonance. The shedding frequency calculation should consider the seabed effect. Traditional models to calculate the natural frequency are oversimplified, and cannot conduct multiple span analyzes. FE analyzes for spanning pipeline are widely adopted in the natural frequency and VIV fatigue analyzes.

4.1.3 | Global buckling analysis

The global buckling of a pipeline appears under the condition that the axial force makes the line deflect to
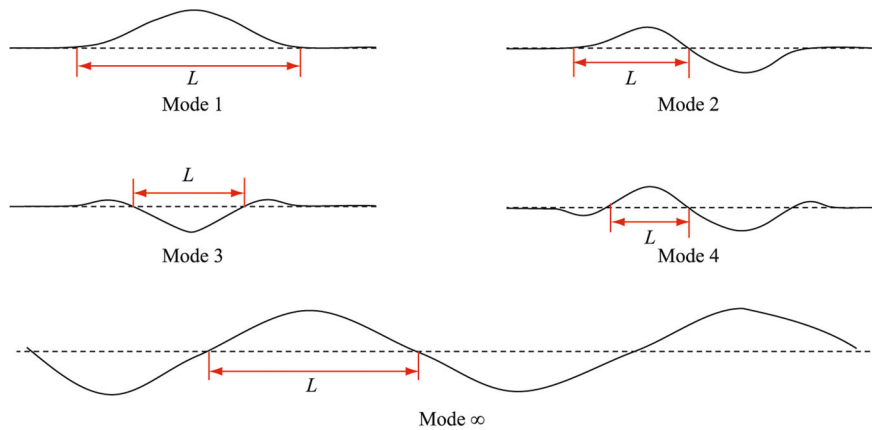
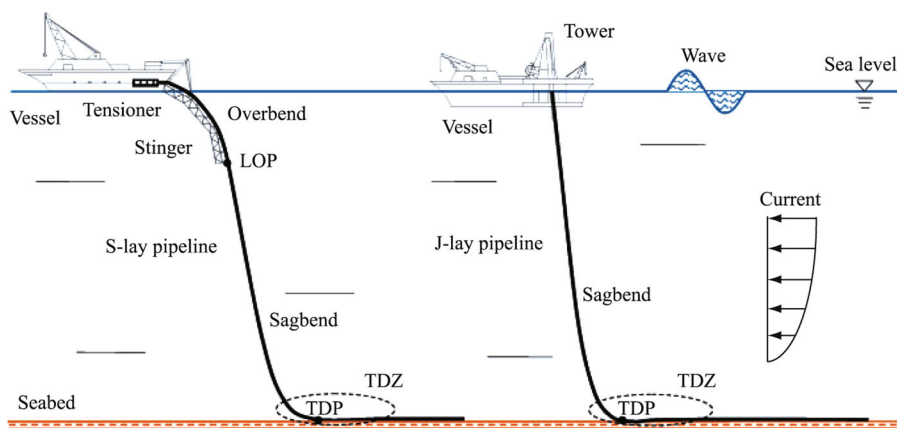**FIGURE 10** Pipeline global buckling modes.

FIGURE 11 Pipe laying methods of the S-lay and J-lay (Xu et al., 2021).

reduce the axial load (Reda & Forbes, 2012). Figure 10 shows different buckling modes. As pipelines work at high temperatures, the buckling probability also increases.

To judge whether the buckling is likely to occur is the first step in the global buckling analysis. Then, whether to prohibit or adapt to buckling is assessed in the following analysis. An approach to prohibit buckling is to add rocks on the pipelines, which cause higher loads in the axial direction. However, if the rock does not offer sufficient constraint, then localized buckling may occur and lead to pipeline failure. Another approach is to adapt to the buckling by allowing the deflect of pipelines. These methods include using a snake lay or buckle mitigation approaches, for example, distributed buoyancies or sleepers. This approach costs less than rock dumping and reduces the pipeline loads, thus becoming more popular.

4.1.4 | Pipeline installation

There are two methods for pipe laying: the J-lay and S-lay, which are conducted by a lay vessel (Wang et al., 2010; Wang et al., 2012; Yuan, Guo, et al., 2012). Figure 11 illustrates the J-lay and S-lay pipe laying (Xu et al., 2021). For the S-lay, the pipe is laid on the seabed with an S-shape. The curvature in the upper part is governed by a supporting structure (stinger). The curvature in touchdown point is governed by the tension on the vessel.

The pipe-lay configuration is analyzed to establish the suitable tension capacity and geometry to avoid the pipe overstress during the installation. Some approaches can be adopted from a catenary shape analysis, which can be treated as approximate solutions. The main aim of the analysis is to check the stress levels in two main regions. The first one is near the stinger where the pipeline is subject to the high bending moment. The controlled curvature demands that the pipeline should be designed with a small factor of safety. The other one is in the sagbend where the pipeline bears bending moments under its self-weight. The curvature in the sagbend changes with the pipeline's axial tension, which cannot be fully controllable.

Another method is the J-lay. The pipeline is manufactured onshore and then reeled onto a huge drum on a special vessel. The pipeline will have plastic deformation during the reeling process. During the installation, the pipe is unreeled and straightened. The pipeline is laid on the seabed with a configuration similar to the J-shape. The assessment of the pipeline-laying approach can be conducted with similar skills. The compatibility of the reeling process should be paid attention to, since the unrecoverable hardening in high-grade steel materials may be caused during the welding process.
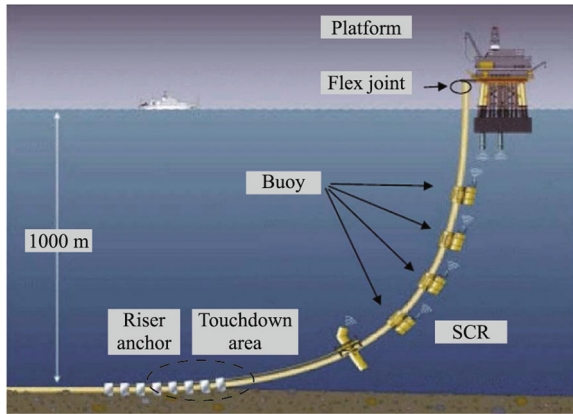
FIGURE 12 Steel catenary risers (SCRs) redrawn from Bai and Bai (2018).

4.2 | Risers

The riser system includes pipelines attached to floaters on the sea surface and wellheads near the seabed. As a fundamental facility for the floating structures to transport oil and gas, the riser is one complex component of a deep-sea production system. Subsea risers can be divided two types: rigid risers and flexible risers. The commonly used risers mainly include steel catenary risers (SCRs), top tensioned risers (TTRs), flexible risers (Bai & Bai, 2018). In this section, steel catenary risers and hybrid risers are to be introduced.

4.2.1 | Steel catenary risers (SCRs)

The SCRs are suitable to the wet tree production in deep water, as shown in Figure 12. The deep-sea SCRs were widely installed in the Gulf of Mexico (GoM). As export lines, SCRs were originally adopted in fixed platforms. Similar to the free-hanging flexible risers, SCRs have horizontal part at the seabed, with an inclined angle of about 20° to the vertical near the fairlead. The riser forms a simple catenary configuration from the platform to the seabed (Hong et al., 2019; Zhou, O'Loughline, et al., 2020). Relative rotations between the platform and the riser can utilise a flex joint to balance the motion. The SCR without intermediate buoys or floating devices is a cost-effective means for oil and gas transport, whereas flexible risers with large diameters display certain economic and technical limitations in this case.

The SCR can compensate for its heave motion by itself, that is, the riser moves up or down onto the seabed. A ball joint is needed for the SCR riser to adjust the rotation caused by currents, waves, and vessel motions. The low-effective tension makes the SCR sensitive to waves and currents. Caused by VIVs, fatigue damage can have a significant inverse impact on the riser. Some devices to suppress VIV, for example, fairing and helical stakes, can maintain the vibrations at an acceptable level.

The riser location may encounter critical conditions, for example, loop currents in the GoM and environmental loads with the main direction in the West of

Africa. In the riser design, vessel motions and offsets should be considered. The metocean data in riser analyzes include water depth, waves, currents, and so forth. For deep water environment conditions, four aspects, namely, extreme storm situations, hydrodynamic loads, soil interaction, and material properties, should be considered in the SCR design (Kopp et al., 2004).

Soil property impact
The inspection of remote-operated vehicles in deep sea indicates that risers would produce complex interaction with the seabed soil near the touchdown zone (TDZ). Riser behavior is significantly affected by soil properties. Soil nonlinear behavior, soil consolidation and remolding, hysteresis, trenching and backfilling, suction effects, and strain rate all exert a certain influence on the loads on the riser. To accurately reproduce the complex interactions is difficult, but modeling those characteristics is important in the assessment of riser stress and fatigue lives. In deep-sea locations, for example, West Africa, the GoM, Brazil, underconsolidated or lightly overconsolidated clays are commonly found in the seabed. However, other soil types can be possible. For example, variable soils are found in glacial areas, for example, in the northwest of the Canada and the Europe. Stiffer clays and sands are often encountered at the seabed.

Floater motion influence
The motions of floaters are determined by the global analysis which takes into account wind, wave, and current loads based on the frequency-domain or time-domain analyzes. The movement data are described by the vessel motions versus time or the response amplitude operators (RAOs). The movements at the riser hang-off position are transferred from the centers of gravity to the floaters. A single riser can be assumed to be a cable under hydraulic loads.

Steel catenary riser design analysis
With the water depth, hang-off angle, and unit weight into consideration, a static configuration can be described according to the catenary theory. Some requirements should be satisfied in the SCR design, for example, SCR diameters, submerged tension on floater, design temperature/pressure, and fluid conditions. Some preliminary analyzes are needed in the design to check whether the extreme response meets the criteria of API-Std-2RD (2020). The extreme rotation for flex joints, required length of strakes (or fairing), and VIV fatigue life are also important. In the detailed design, some installation and special analyzes are of necessity, for example, the VIV fatigue analysis, the coupled system analysis.

4.2.2 | Flexible risers

Figure 13 shows the sketch of flexible risers. Flexible risers originated from the work conducted in the 1970s. At the beginning, flexible pipes were adopted in the mild environments, for example, the Far East, offshore Brazil,
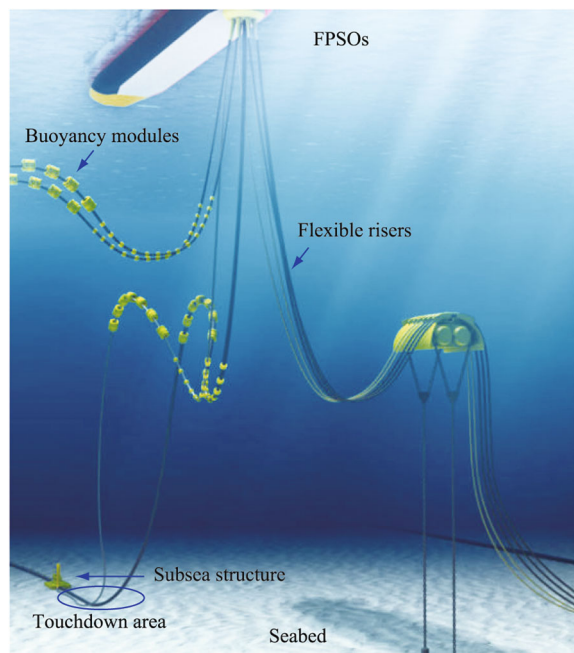
FIGURE 13 Flexible risers redrawn from www.aisltd.com/application/.

FIGURE 14 Suction anchors (www.oedigital.com/news/478844).

and the Mediterranean (Bai & Bai, 2018). Then, the flexible pipe technology experienced a rapid development. Flexible pipes can be adopted in deep water, high pressure, high temperature. In adverse weather conditions, flexible pipes also have the ability to adapt to large vessel movements.

Compared with the axial stiffness, the low bending stiffness is a main feature of a flexible pipe. This feature is achieved by adopting various layers with different materials in the pipe manufacture. These layers can slip past each other when subjected to internal and external loads, which leads to its low bending stiffness. The steel armor layers with high stiffness are combined to ensure its strength, while the polymer sealing layers increase the fluid integrity due to its low stiffness. This method of pipe manufacturing provides some advantages, for example, easy prefabrication, convenient storage on reels, lower transport and installation costs, and suitability with other structures. Five main factors contributing to the flexible riser failure are pressure, temperature, product fluid composition, ancillary components, and service loads, which should be carefully handled in the design (Elman & Alvim, 2008).

4.3 | Brief summary

Subsea pipelines and risers have some different problems due to their different configurations. For the subsea pipelines, the on-bottom stability, free-span analysis, and global buckling should be assessed, which are closely related to soil–structure interaction and pipeline stress state. For the risers, for example, SCR, the fatigue damage induced by VIVs can be fatal, which is related to soil resistance and floater motion. Flexible risers have developed rapidly, which can be adopted in deep water environments with high pressure and high temperature.
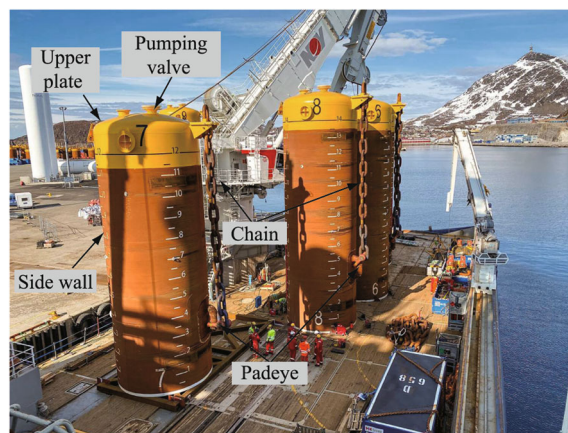
5 | DEEP-SEA ANCHORS

This section is focused on the deep-sea anchors, including suction anchor, fluke anchor, suction-embedded plate anchor (SEPLA), and dynamically installed anchor (DIA). The installation and capacity analyzes of each anchor are introduced to show their application in different soils. The impact of seabed trenches on the anchors is then analyzed particularly.

5.1 | Suction anchor

Widely used in deep sea, suction anchor is a steel barrel structure, with a closed upper plate and an open on the bottom, as shown in Figure 14 (Guo et al., 2018; Zhou, Guo, Wang, Zhang, et al., 2021). The diameters of suction anchors are commonly among 4–8 m, sometimes larger than 8 m. The ratio of length to diameter is generally between 3 and 6.

5.1.1 | Anchor installation

A suction anchor is installed by the inner suction inside the caisson (Fu et al., 2021; Guo et al., 2012; Zhao et al., 2022). Some pumps work to maintain the suction inside the anchor. Under the condition, a seepage field will be formed, which reduces the effective soil stress inside the anchor and the anchor tip resistance (Guo et al., 2017; Shen et al., 2019). The anchor can be installed in sand, clay, and silt. In clay, the penetration resistance along the skirt wall can be calculated according to Andersen and Jostad (2004), and Houlsby and Byrne (2005a). Houlsby and Byrne (2005b) proposed a method to determine the penetration resistance in sand. For the anchor installation, it is beneficial to suppress the development of soil heave by applying the intermittent suction (Guo et al., 2012).

5.1.2 | Capacity analysis

Suction anchors are widely adopted in the clay and sand seabed. The bearing capacities in clay have been studied

based on experiments and numerical methods (Andersen et al., 2005; Aubeny et al., 2003; Byrne & Houlsby, 2002; Guo et al., 2018; House & Randolph, 2001; Liu et al., 2013; Rao et al., 2006). House and Randolph (2001) developed an upper bound approach with horizontal or rotation components, and verified the method accuracy with semi-analytical FE results. Byrne and Houlsby (2002) conducted a series of model tests at different rates to investigate the vertical capacity, and revealed the failure modes. Aubeny et al. (2003) proposed a method to estimate the horizontal capacity based on an upper bound plasticity formulation. Liu et al. (2013) constructed the force equilibrium equations, and proposed a method to calculate anchor capacity considering different loading angles. Guo et al. (2018) carried out a series of model tests to investigate the capacities and the failure modes in clay, and found the caisson's failure mode mainly depends on the loading angle.

Some studies about the suction anchor capacity were focused on sand (Bang et al., 2011; Deng & Carter, 2000; Gao et al., 2013; Jang & Kim, 2013; Liu et al., 2015; Zhou, Guo, Wang, Zhang, et al., 2021). Bang et al. (2011) conducted centrifuge model tests to obtain the suction anchor capacity in sand, and proposed an analytical solution of anchor horizontal pull-out capacity. Jang and Kim (2013) found that the equation derived from Rankine passive earth pressure has a good prediction of the test results based on centrifuge model tests. Liu et al. (2015) proposed an analytical model to predict the anchor capacity to calculate the failure surface angle based on the minimum force principle. Rui et al. (2022) conducted a series of centrifuge model tests to investigate the trench influence on the anchor capacity in the carbonate sand (Rui et al., 2020), and revealed the trench influences the anchor failure mode.

5.2 | Fluke (drag) anchor

Fluke (drag) anchor is a type of drag-embedded anchor, mainly including anchor plate (fluke), shank (Zhou

et al., 2020) (Figure 15). The fluke anchor is installed by drag embedment.

5.2.1 | Anchor installation

The installation of fluke anchor is closely related to the angle of fluke and shank. For the sand or stiff clay, the recommended fluke-shank angle is 32°, while the recommended angle is 50° for soft clay. During the installation, the drag anchor is placed on the seabed and has a certain initial embedded depth. Then, the anchor is pulled into the seabed by applying the pretension on the mooring line to reach a set depth. In different types of seabed soils, the drag distance can reach 10–20 times the plate length, and the penetration depth can reach one to five times the plate length. Vessel movement and winching of the mooring line are the two main installation methods (Wang et al., 2014).

5.2.2 | Capacity analysis

The holding capacity of fluke anchor is dependent on the penetration depth, thus the assessment of anchor final depth is of significance (Liu et al., 2010; Zhang et al., 2022). The pull-out capacity of fluke anchor originates from the bearing resistance produced by the fluke, which is related to the penetration depth, soil properties, anchor size, and so forth. Two basic problems are related to the calculation of fluke anchor capacity: (1) the anchor trajectory during installation and (2) the anchor orientation after installation. The anchor trajectory influences the final embedment depth, mainly depending on the soil properties. The anchor fluke-shank angle is determined according to the soil type, and it also determines the final orientation. The trajectory and capacity of drag anchors have been well investigated considering the constant and linearly changing strength profiles by analytical methods (Aubeny & Chi, 2010; Bransby & O'Neill, 2020; Neubecker & Randolph, 1996; Peng & Liu, 2019) and experimentally (Dunnavant & Kwan, 1993; O'Loughlin et al., 2006). However, the layered soils increase uncertainties
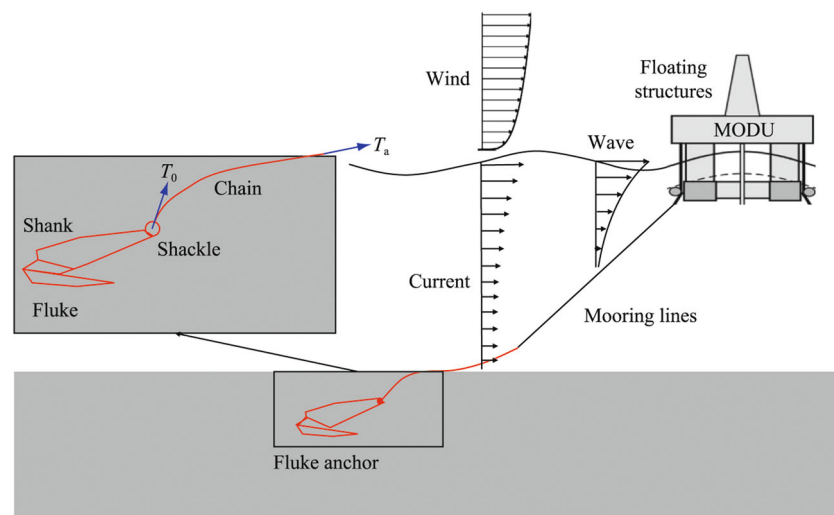

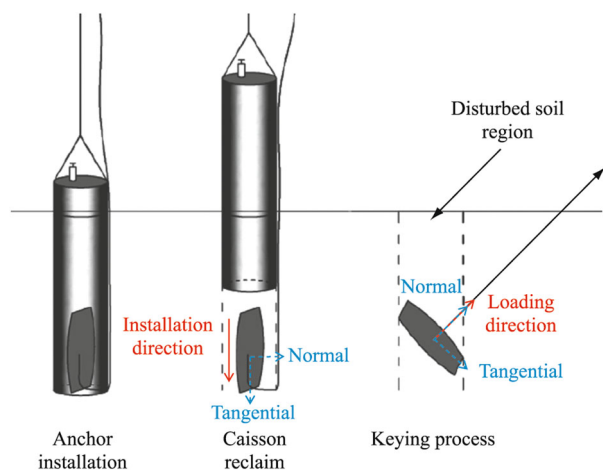**FIGURE 15** Fluke anchor configurations.

FIGURE 16 Installation and service status of suction-embedded plate anchor.

to fluke anchor trajectory prediction as well as its capacity calculation.

5.3 | SEPLA

SEPLA is a kind of plate anchor with the installation assisted by the suction caisson, as shown in Figure 16. Compared with other anchors, SEPLA is featured with a relatively high bearing efficiency (Rui et al., 2023).

5.3.1 | Anchor installation

Before installation, the SEPLA is fixed on the bottom of the suction caisson and accurately positioned in the seabed (Gaudin et al., 2006). The caisson can be reclaimed after the anchor installation. SEPLA rotates under the pretension loads, called as "keying process," until the mooring line is almost perpendicular to the anchor plate (Wang et al., 2011). The complex keying process and bearing capacity can be studied through model tests, large deformation FE analyzes, and plastic analyzes. Gaudin et al. (2006) investigated the keying process and the anchor capacity of SEPLA, and found that the anchor embedment suffers a certain loss during the keying process. For large deformation FE simulation, Zhao and Liu (2014) adopted the Coupled Eulerian-Lagrangian (CEL) method to analyze the process of anchor installation considering the impact of mooring line on the anchor trajectory. The plastic analysis based on the yield envelope is a macro element model, which can effectively predict the behaviors during the keying process (Yang et al., 2012).

5.3.2 | Capacity analysis

When SEPLA rotates to fully resist the vertical loads, the failure mechanism of SEPLA is easier to analyze, as shown in Figure 17. In the limited state, if the soil failure region extends to the surface, the anchor plate is shallowly embedded. If soil failure only occurs in the
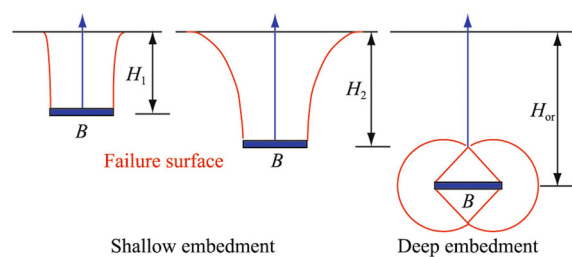

FIGURE 17 Plate anchor failure modes in seabed.

local region around the anchor plate, the anchor plate is defined as deeply embedded anchor. In clay, when the anchor sizes are fixed, the anchors have a critical depth H_{cr}. When the anchor plate depth reaches H_{cr}, the soil flow is around the anchor plate. With the increasing embedment depth, the bearing capacity remains unchanged (Guo et al., 2023; Guo, Nian, et al., 2022; Merifield et al., 2001). Based on the assumption that the anchor plate and soil have no separation, Rowe et al. (1978) developed the upper bound method to obtain the bearing capacity coefficient of the deep embedded anchor plate in homogeneous clay.

5.4 | DIAs

DIAs penetrate into the seabed by its kinetic energy. As shown in Figure 18, DIAs contain various types, such as torpedo anchor, OMNI-Max, dynamically embedded plate anchor, light-weight gravity installed plate anchor and DPAIII (Han & Liu, 2020). Among these anchors, the torpedo anchor is mostly used in engineering due to its simple configuration, cheap and easy installation.

5.4.1 | Anchor installation

The installation process of DIAs is as follows. First, the torpedo anchor is released at a certain height (about 30–150 m) above the seabed. Then, it falls freely and accelerates in the water, and finally penetrates the seabed to a certain depth by its kinetic energy. Since the DIA installation does not need special equipment, its application is not limited by water depth. Two methods are usually adopted to simulate the dynamic installation process, namely, the large deformation FE method and CFD method (Han & Liu, 2020). Based on the simulations, parameter studies have been carried out to explore the influence of various factors on the final penetration depth of DIAs. These factors include impact velocity, anchor weight and shape, soil strength, anchor-soil contact characteristics, and so forth.

5.4.2 | Capacity analysis

At present, there are two main methods to calculate the uplift bearing capacity of piles or anchors in service (Richardson, 2008): the American Petroleum Institute Method (API) method (API RP 2A-WSD R2006, 2006)
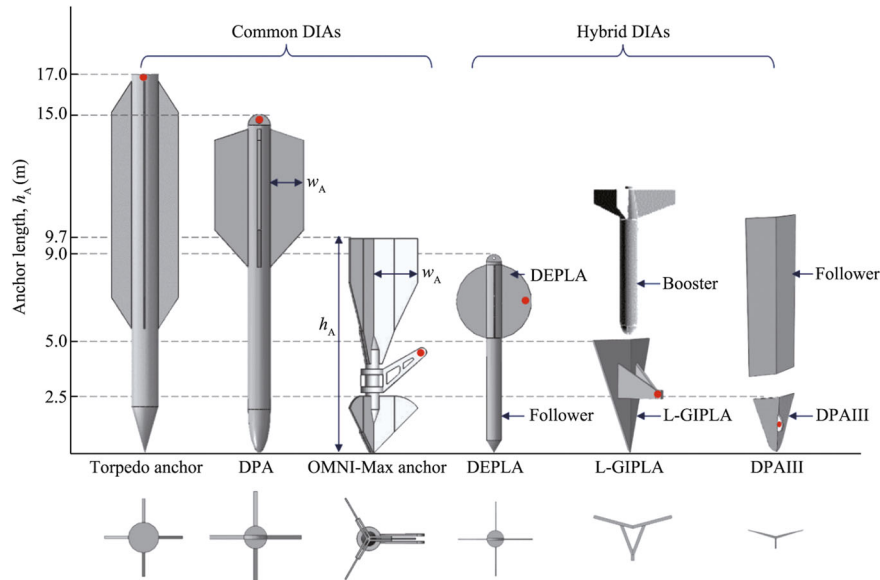
FIGURE 18 Sketches of dynamically installed anchor (DIA) (Han & Liu, 2020). DEPLA, dynamically embedded plate anchor; L-GIPLA, lightweight gravity installed plate anchor.

and the Marine Technology Directorate (MTD) method. Among them, the API method assumes that the failure mode of the torpedo anchor is similar to that of the end bearing friction pile. The uplift bearing capacity of torpedo anchor consists of three parts: anchor weight, friction between anchor and soil, and end bearing capacity of anchor end. Physical model tests, field tests, and centrifuge model tests were conducted to explore the interaction between anchors and seabed soils (Han et al., 2019; O'Loughlin et al., 2014). O'Loughlin et al. (2004) found that adding side wings increases the contact area between soil and anchor, thus improving the bearing capacity of torpedo anchors. Richardson (2008) revealed that two peaks appear in the anchor loading process with displacement, which is caused by the unsynchronized development of the interface friction and the anchor end resistance. O'beirne et al. (2015) carried out a series of pull-out tests using small-scale torpedo anchors, and found that the uplift bearing capacity of torpedo anchor is greatly affected by the load angles.

5.5 | Trench near anchors

5.5.1 | Trench impact on anchors

The seabed trenches have inverse impacts on the anchor capacity, for example, reducing the anchor capacities (Alderlieste et al., 2016; Arslan et al., 2015; Feng et al., 2019; Gao et al., 2022; Hernandez-Martinez et al., 2015; Rui, Guo, Wang, Zhou, et al., 2022). Hernandez-Martinez et al. (2015) investigated the anchor capacity with the existence of a trench near a suction anchor, and found anchor capacity exhibits a reduction depending on the loading angles. Arslan et al. (2015) found that the trench impact on the passive suction at the anchor bottom is limited without the seepage path around the anchor. Based on FE simulation, Feng et al. (2019) found that the trench width

has a great impact on the anchor capacity. Rui, Guo, Wang, Wang, et al. (2022) conducted a series of centrifuge model tests to investigate the trench impact on the anchor capacity in carbonate sand (Rui, Guo, Si, et al., 2021), and found that due to the impact of the trenches, the anchor failure mechanism changes from the translational movement to the forward rotation, and the anchor capacity decreases accordingly.

5.5.2 | Trench formation

The trench formation is a complex process involving the chain movement, soil erosion, soil remolding and consolidation, soil collapse and removal, among which the chain-seabed interaction is the trigger factor (Rui, Guo, Wang, Duo, et al., 2022; Rui, Guo, Wang, et al., 2021; Sassi et al., 2017; Versteele et al., 2017). For chain-soil tangential interaction, Rui, Wang et al. (2020), Rui, Wang, Guo, Zhou et al. (2021); Rui, Wang, Guo, Zhang et al. (2021) designed a chain–soil interaction apparatus to measure the chain axial resistances, and proposed a new expression of chain axial resistance to predict the chain profile in sand. Rui, Guo, Wang, Duo et al. (2022) established a framework to calculate the axial soil resistance from three components. In fact, trench formation is much more complex than chain–seabed interaction (O'neill et al., 2018). To simulate trench formation, Sassi et al. (2017) carried out centrifuge model tests to simulate the trench formation, and found that the chain movement under the cyclic loads is a key factor. Based on the static finite difference method, Versteele et al. (2017) proposed a two-dimensional (2D) model to simulate the trench evolution. Based on large deformation FE approach, Sun et al. (2020) established a numerical model to simulate the trench formation. Similarly, with the FE method, Wang, Rui et al. (2020) and Rui, Guo, Si et al. (2020)

established a 2D trench profile prediction method which takes the mooring line-soil dynamic interaction into account. However, the detailed process of soil remolding and consolidation, soil collapse and removal are not considered in the above studies.

5.6 | Brief summary

Deep-sea anchors, for example, suction anchor, fluke anchor, SEPLA, and DIA, have different installation methods and bearing capacity efficiencies. The installation and capacity analyzes of anchors should give full consideration to the soil types. For instance, final penetration depths should be considered when adopting fluke anchor and DIA in the sand seabed. The anchor selection should consider the fabrication, transportation, installation, and so forth. In addition, the seabed trench impact on the anchor is assessed in long-term service, and the trench formation is found to be closely related to the chain movement, soil erosion, soil remolding and consolidation, soil collapse and removal.

6 | SUMMARY

This study provided a brief introduction about seabed structures and foundations related to deep-sea resource development. First, the floating structures were introduced, and the sea environment loads were briefly analyzed. Second, the subsea production structures, including subsea manifolds and their foundations (mudmats, suction piles) were introduced. Third, the basic characteristics and design methods of deep-sea pipelines, including subsea pipeline and risers, were analyzed in detail. The fourth part placed its focus on the deep-sea anchors. The installation and bearing capacity were presented accordingly. The seabed trenches were found to influence the anchor capacity, which was particularly analyzed. The main findings are as follows:

1. The floating structures mainly have four types, which adapt to the different environmental conditions and design requirements. Spar platforms adopt to relatively deep water, and TLP platforms need larger mooring line tension. Semi-submersible platforms are easier to be installed, and FPSOs are the most flexible ones in practice. Environment loads, for example, wind, wave, current, are the inputs for offshore structure design. The accurate calculation of loads is necessary for further structure design.

2. Subsea production structures are important components at the seabed to transport oil & gas. A subsea manifold system mainly consists of a manifold, a foundation and a supporting structure. Manifold foundation includes the mudmat with small aspect ratio and suction pile with large embedded depth. For the mudmat, the overturning and bearing capacity should be assessed. For suction piles, the bearing capacity and installation resistance should be carefully designed.

3. Subsea pipelines and risers have some different problems due to their different configurations. For the subsea pipelines, the on-bottom stability, free-span analysis, and global buckling should be assessed, which are closely related to soil–structure interaction and pipeline stress state. For the risers, for example, SCR, the fatigue damage induced by VIVs can be fatal, which is related to soil resistance and floater motion. Flexible risers have developed rapidly, which can be adopted in deep water environments with high pressure and temperature.

4. Four types of anchors in the deep-sea region are introduced from the aspects of installation and bearing capacity. The suction anchor and SEPLA are installed with the assistance of the suction, fluke anchor by drag embedment, and DIAs by its kinetic energy. For the capacity, different anchors have their failure mechanisms based on the soil properties and load conditions. In addition, the seabed trench impact on the anchor is assessed in long-term service, and the trench formation is found to be closely related to the chain movement, soil erosion, soil remolding and consolidation, soil collapse and removal.

This study provided a brief introduction about seabed structures and foundations mainly from the perspective of engineering design and pointed out the research gaps and further research directions.

7 | LIMITATION

This paper fails to present detailed information due to space limitations. The involved mechanics, especially structural mechanics, fluid mechanics, and geotechnical mechanics, have not been thoroughly analyzed and explored. This paper presents some design methods and equations, but the final power of interpretation still lies in the cited standards and design codes.

CONFLICT OF INTEREST STATEMENT
The authors declare no conflict of interest.

DATA AVAILABILITY STATEMENT
The data that support the findings of this study are available from the first author (Shengjie Rui), upon reasonable request.

ORCID
Shengjie Rui http://orcid.org/0000-0002-0779-3598
Kanmin Shen http://orcid.org/0000-0003-1965-7400

REFERENCES

Agarwal AK, Jain AK. Dynamic behavior of offshore spar platforms under regular sea waves. *Ocean Eng.* 2003;30(4):487-516.

Alderlieste E, Romp R, Kay S, Lofterød A. Assessment of seafloor trench for suction pile moorings: a field case. In: *Proceedings of Offshore Technology Conference (OTC)*. OTC-27035-MS; 2016.

Andersen KH, Murff JD, Randolph MF, et al. Suction anchors for deep water applications. In: *Proceedings of International Symposium on Frontiers in Offshore Geotechnics*, 2005.

Andersen KH, Jostad HP. Shear strength along inside of suction anchor skirt wall in clay. In: *Offshore Technology Conference*. OTC-16844-MS; 2004.

Andersen KH, Jostad HP. Foundation design of skirted foundations and anchors in clay. In: *Offshore Technology Conference (OTC)*. OTC-10824-MS; 1999.

API-RP-2A-WSD (R2006). *Design of Risers for Floating Production Systems (FPSs) and Tension-Leg Platforms (TLPs)*; 2006.

API-Std-2RD (R2020). *Dynamic Risers for Floating Production Systems*. 2nd ed.; 2020.

API-RP-2A-WSD (R2020). *Recommended Practice for Planning, Designing and Constructing Fixed Offshore Platforms-Working Stress Design*; 2020.

Arslan H, Peterman BR, Wong PC, Bhattacharjee S. Remaining capacity of the suction pile due to seabed trenching. Presented at: the International Ocean and Polar Engineering Conference; 2015.

Aubeny CP, Han SW, Murff JD. Inclined load capacity of suction caissons. *Int J Numer Anal Methods in Geomech.* 2003;27(14):1235-1254.

Aubeny CP, Chi C. Mechanics of drag embedment anchors in a soft seabed. *J Geotech Geoenviron Eng.* 2010;136(1):57-68.

Bachynski EE, Moan T. Design considerations for tension leg platform wind turbines. *Mar Struct.* 2012;29(1):89-114.

Bai Y, Bai Q. *Subsea Engineering Handbook*. Gulf Professional Publishing; 2018.

Bang S, Jones KD, Kim KO, Kim YS, Cho Y. Inclined loading capacity of suction piles in sand. *Ocean Eng.* 2011;38(7):915-924.

Boesch DF, Rabalais NN. *Long-Term Environmental Effects of Offshore Oil and Gas Development*. Elsevier Applied Science; 1987.

Bransby MF, O'Neill MP. Drag anchor fluke-soil interaction in clays. In: *Numerical Models in Geomechanics*. CRC Press; 2020:489-494.

Byrne BW, Houlsby GT. Experimental investigations of response of suction caissons to transient vertical loading. *J Geotechn Geoenviron Eng.* 2002;128(11):926-939.

Colliat JL. Anchors for deepwater to ultra-deepwater moorings. Offshore technology conference OTC-14306, Houston, TX; 2002.

Cordes EE, Jones DOB, Schlacher TA, et al. Environmental impacts of the deep-water oil and gas industry: a review to guide management strategies. *Front Environ Sci.* 2016;4:58.

Deng W, Carter JP. Inclined uplift capacity of suction caissons in sand. In: *Proceedings of Offshore Technology Conference*; 2000:500–506.

DNV. Foundations, Classification Notes No. 30.4; 1992.

Duggal A, Minnebo J. The floating production, storage and offloading system–past, present and future. In: *Offshore Technology Conference*. OTC-30514-MS; 2020.

Dunnavant T, Kwan CT. Centrifuge modelling and parametric analyses of drag anchor behavior. Offshore technology conference; Houston, TX; 1993.

Elman P, Alvim R. Development of a failure detection system for flexible risers. 18th international offshore and polar engineering conference. ISOPE-I-08-299; 2008.

Eltaher A, Rajapaksa Y, Chang KT. Industry trends for design of anchoring systems for deepwater offshore structures. Offshore technology conference OTC 15265, Houston, TX; 2003.

Feng X, Gourvenec S, White DJ. Load capacity of caisson anchors exposed to seabed trenching. *Ocean Eng.* 2019;171:181-192.

Fu D, Zhou Z, Yan Y, Pradhan DL, Hennig J. A method to predict the torsional resistance of suction caisson with anti-rotation fins in clay. *Mar Struct.* 2021;75:102866.

Gao Y, Qiu Y, Li B, Li D, Sha C, Zheng X. Experimental studies on the anti-uplift behavior of the suction caissons in sand. *Appl Ocean Res.* 2013;43:37-45.

Gao Y, Qu L, Wang L, Guo Z. Experimental study on the sandy seabed trench development of the catenary mooring chain at touchdown zone. *Ocean Eng.* 2022;264:112470.

Gaudin C, O'Loughlin CD, Randolph MF, Lowmass AC. Influence of the installation process on the performance of suction-embedded plate anchors. *Géotechnique.* 2006;56(6):381-391.

Gausland I. *Seismic Surveys Impact on Fish and Fisheries*. Norwegian Oil Industry Association (OLF); 2003.

Gonçalves RT, Rosetti GF, Fujarra ALC, Oliveira AC. Experimental study on vortex-induced motions of a semi-submersible platform with four square columns, Part II: effects of surface waves, external damping and draft condition. *Ocean Eng.* 2013;62:10-24.

Guo X, Liu Z, Zheng J, Luo Q, Liu X. Bearing capacity factors of T-bar from surficial to stable penetration into deep-sea sediments. *Soil Dyn Earthq Eng.* 2023;165:107671.

Guo X, Nian T, Zhao W, et al. Centrifuge experiment on the penetration test for evaluating undrained strength of deep-sea surface soils. *Int J Mining Sci Technol.* 2022;32(2):363-373.

Guo X, Stoesser T, Nian T, Jia Y, Liu X. Effect of pipeline surface roughness on peak impact forces caused by hydrodynamic submarine mudflow. *Ocean Eng.* 2022;243:110184.

Guo Z, Jeng D, Guo W, He R. Simplified approximation for seepage effect on penetration resistance of suction caissons in sand. *Ships Offshore Struct.* 2017;12(7):980-990.

Guo Z, Jeng DS, Guo W, Wang L. Failure mode and capacity of suction caisson under inclined short-term static and one-way cyclic loadings. *Mar Georesources Geotechnol.* 2018;36(1):52-63.

Guo Z, Jeng DS, Zhao H, Guo W, Wang L. Effect of seepage flow on sediment incipient motion around a free spanning pipeline. *Coast Eng.* 2019;143:50-62.

Guo Z, Wang L, Yuan F, Li L. Model tests on installation techniques of suction caissons in a soft clay seabed. *Appl Ocean Res.* 2012;34:116-125.

Hafez KA, Abdelsalam MA, Abdelhameed AN. Dynamic on-bottom stability analysis of subsea pipelines using finite element model-based general offshore analysis software: a case study. *Beni-Suef Univer J Basic Appl Sci.* 2022;11(1):36.

Han C, Liu J. A review on the entire installation process of dynamically installed anchors. *Ocean Eng.* 2020;202:107173.

Han C, Liu J, Zhang Y, Zhao W. An innovative booster for dynamic installation of OMNI-Max anchors in clay: physical modelling. *Ocean Eng.* 2019;171:345-360.

Hernandez-Martinez FG, Saue M, Schroder K, Jostad HP. Trenching effects on holding capacity for in-service suction anchors in high plasticity clays. In: *SNAME 20th Offshore Symposium*. SNAME-TOS-2015-020; 2015.

Hong Z, Fu D, Zhou Z, Liu W, Yan Y. Modelling nonlinear time-dependent pipeline walking induced by SCR tension and downslope. *Appl Ocean Res.* 2019;93:101949.

Houlsby GT, Byrne BW. Design procedures for installation of suction caissons in clay and other materials. *Proc Inst Civil Eng Geotech Eng.* 2005;158(2):75-82.

Houlsby GT, Byrne BW. Design procedures for installation of suction caissons in sand. *Proc Inst Civil Eng Geotech Eng.* 2005;158(3):135-144.

House AR, Randolph MF. Installation and pull-out of stiffened suction caissons in cohesive sediments. Proceedings of the 11th international offshore and polar engineering conference. ISOPE-I-01-212; 2001.

Hyne NJ. *Nontechnical Guide to Petroleum Geology, Exploration, Drilling and Production*. PennWell; 2001.

Jang YS, Kim YS. Centrifugal model behavior of laterally loaded suction pile in sand. *KSCE J Civil Eng.* 2013;17(5):980-988.

Kark S, Brokovich E, Mazor T, Levin N. Emerging conservation challenges and prospects in an era of offshore hydrocarbon exploration and exploitation. *Conserv Biol.* 2015;29:1573-1585.

Kopp F, Light BD, Preli TS, Rao VS, Stingl KH. Design and installation of the Na Kika export pipelines, flowlines and risers. Offshore technology conference OTC 16703, Houston, TX; 2004.

Liu H, Pisanò F, Jostad HP, Sivasithamparam N. Impact of cyclic strain accumulation on the tilting behaviour of monopiles in sand: an assessment of the Miner's rule based on SANISAND-MS 3D FE modelling. *Ocean Eng.* 2022;250:110579.

Liu H, Sivasithamparam N, Suzuki Y, Jostad HP. Load history idealisation effects for design of monopiles in clay. *Géotechnique*. 2022:1-11.

Liu H, Zhang W, Zhang X, Liu C. Experimental investigation on the penetration mechanism and kinematic behavior of drag anchors. *Appl Ocean Res*. 2010;32(4):434-442.

Liu H, Peng J, Zhao Y. Analytical study of the failure mode and pullout capacity of suction anchors in sand. *Ocean Syst Eng*. 2015;5(4):279-299.

Liu H, Wang C, Zhao Y. Analytical study of the failure mode and pullout capacity of suction anchors in clay. *Ocean Syst Eng*. 2013;3(2):79-95.

Ma K-T, Luo Y, Kwan C-TT, Wu Y. *Mooring System Engineering for Offshore Structures*. Gulf Professional Publishing; 2019.

Merifield RS, Sloan SW, Yu HS. Stability of plate anchors in undrained clay. *Géotechnique*. 2001;51(2):141-153.

Morse TL, Mathierson E, Shrestha P. *The Dangers of Flood Scouring on Buried Pipeline River Crossings. Exponent Engineering and Scientific Consulting*; 2017.

Murawski SA, Hollander DJ, Gilbert S, Gracia A. Deepwater oil and gas production in the Gulf of Mexico and related global trends. *Scenarios and Responses to Future Deep Oil Spills*. Springer; 2020:16-32.

Rao SN, Latha KH, Pallavi B, Surendran S. Studies on pull-out capacity of anchors in marine clays for mooring systems. *Appl Ocean Res*. 2006;28:103-111.

Neubecker SR, Randolph MF. The performance of drag anchor and chain systems in cohesive soil. *Marine Georesources Geotechnol*. 1996;14(2):77-96.

Niedzwecki JM, Huston JR. Wave interaction with tension leg platforms. *Ocean Eng*. 1992;19(1):21-37.

Nur Fatmala-15512050 Ocean Engineering ITB. www.ocean.itb.ac.id

O'beirne C, O'Loughlin CD, Wang D, Gaudin C. Capacity of dynamically installed anchors as assessed through field testing and three-dimensional large-deformation finite element analyses. *Can Geotech J*. 2015;52(5):548-562.

O'Loughlin CD, Blake AP, Richardson MD, Randolph MF, Gaudin C. Installation and capacity of dynamically embedded plate anchors as assessed through centrifuge tests. *Ocean Eng*. 2014;88:204-213.

O'Loughlin CD, Lowmass A, Gaudin C, Randolph MF. Physical modelling to assess keying characteristics of plate anchors. In: *Proceedings of the 6th International Conference on Physical Modelling in Geotechnics* (Vol. 1, 659-665); 2006.

O'Loughlin CD, Randolph MF, Richardson MD. Experimental and theoretical studies of deep penetrating anchors. Proceedings offshore technology conference OTC 16841, Houston, TX; 2004.

O'neill M, Erbrich C, Mcnamara A. Prediction of seabed trench formation induced by anchor chain motions. In: *Proceedings of Offshore Technology Conference*. OTC-29068-MS; 2018.

Peng J, Liu H. Analytical study on comprehensive behaviors of drag anchors in the seabed. *Appl Ocean Res*. 2019;90:101855.

Reda A, Forbes G. Investigation into the dynamic effects of lateral buckling of high temperature/high-pressure offshore pipelines. Proceedings of acoustics 2012-fremantle; 2012.

Rho YH, Kim K, Jo CH, Kim DY. Static and dynamic mooring analysis–stability of floating production storage and offloading (FPSO) risers for extreme environmental conditions. *Int J Nav Archit Ocean Eng*. 2013;5(2):179-187.

Richardson MD. Dynamically installed anchors for floating offshore structures. Doctoral dissertation. University of Western Australia; 2008.

Rose B. *Flowline Tie-in Systems, SUT Subsea Awareness Course*; 2008.

Rowe CR, Patel D, Southmayd WW. The Bankart procedure: a long-term end-result study. *J Bone Joint Surg*. 1978;60(1):1-16.

Rui S, Guo Z, Wang L, Dou Y, Zhou W, Zha X. Mobilization mechanism and calculation method of embedded chain axial resistance in sand. *Ocean Eng*. 2022;263:112356.

Rui S, Guo Z, Wang L, Liu H, Zhou W. Numerical investigations on load transfer of mooring line considering chain-seabed dynamic interaction. *Mar Georesources Geotechnol*. 2021;39(12):1433-1448.

Rui S, Guo Z, Wang L, Wang H, Zhou W. Inclined loading capacity of caisson anchor in South China Sea carbonate sand considering the seabed soil loss. *Ocean Engineering*. 2022;260:111790.

Rui S, Guo Z, Wang L, Zhou W, Li YJ, Shen KM. Tangential shear behavior between sands and mooring chain. In: *Proceeding of International Symposium on Frontiers in Offshore Geotechnics*, August 16–19, 2020.

Rui S, Wang L, Shen K, Guo Z, Zhou W, Li Y. Numerical studies on seabed trench formation near the mooring foundation for floating wind turbines. In: *Proceeding of International Offshore and Polar Engineering Conference*, October 11–16, ISOPE-I-20-2208; 2020.

Rui S, Guo Z, Si TL, Li YJ. Effect of particle shape on the liquefaction resistance of calcareous sands. *Soil Dyn Earthq Eng*. 2020;137:106302.

Rui S, Guo Z, Si TL, Zhou WJ, Zha X. Particle shape influence on the deformation resistance of carbonate sands under drained condition. *Soil Dyn Earthq Eng*. 2021;144:106688.

Rui S, Wang LZ, Guo Z, Cheng XM, Wu B. Monotonic behavior of interface shear between carbonate sands and steel. *Acta Geotechn*. 2021;16:167-187.

Rui S, Wang LZ, Guo Z, Hua Y, Zhou WJ. Axial interaction between anchor chain and sand. Part II: cyclic loading test. *Appl Ocean Res*. 2021;114(6):102815.

Rui S, Wang LZ, Guo Z, Zhang HJ, Zhou WJ. Axial interaction between anchor chain and sand. Part I: monotonic loading test. *Appl Ocean Res*. 2021;113(1):102761.

Rui S, Wang LZ, Guo Z, Zhou WJ, Li YJ. Cyclic behavior of interface shear between carbonate sands and steel. *Acta Geotech*. 2021;16:189-209.

Rui S, Zhou WJ, Guo Z, Shen KM. A review on seabed trench induced by mooring line dynamics and anchor foundation bearing capacity. *J Mar Sci Appl*. 2023;2:1-15.

Sahu C, Kumar R, Sangwai JS. Comprehensive review on exploration and drilling techniques for natural gas hydrate reservoirs. *Energy Fuels*. 2020;34(10):11813-11839.

Sassi K, Kuo MYH, Versteele H, Cathie DN, Zehzouh S. Insights into the mechanisms of mooring line trench formation. Presented at: the Offshore Site Investigations and Geotechnics Conference, Society for Underwater Technology, September 10-12, 2017, SUT OSIG, London, UK; 2017.

Shen K, Guo Z, Wang L, Rui S, He B. Investigation on seepage erosion and safety mechanism of suction caisson installation. In: *Proceedings of the 1st Vietnam Symposium on Advances in Offshore Engineering: Energy and Geotechnics*. Springer Singapore; 2019:196-202.

Sun C, Bransby MF, Neubecker SR, Randolph MF, Feng X, Gourvenec S. Numerical investigations into development of seabed trenching in semitaut moorings. *J Geotechn Geoenviron Eng*. 2020;146(10):04020098.

Versteele H, Kuo MYH, Cathie DN, Sassi K, Zehzouh S. Mooring line trenching-numerical simulation of progressive erosion. Presented at: the Offshore Site Investigations and Geotechnics Conference, Society for Underwater Technology, September 10-12, 2017, SUT OSIG, London, UK; 2017.

Wang L, Rui S, Guo Z, Gao Y, Zhou W, Liu Z. Seabed trenching near the mooring anchor: history cases and numerical studies. *Ocean Eng*. 2020;218:108233.

Wang D, Hu Y, Randolph MF. Keying of rectangular plate anchors in normally consolidated clays. *J Geotechn Geoenviron Eng*. 2011;137(12):1244-1253.

Wang L, Shen K, Li L, Guo Z. Integrated analysis of drag embedment anchor installation. *Ocean Eng*. 2014;88:149-163.

Wang L, Yuan F, Guo Z, Li L. Numerical analysis of pipeline in J-lay problem. *J Zhejiang Univ Sci A*. 2010;11:908-920.

Wang LZ, Yuan F, Guo Z, Li LL. Analytical prediction of pipeline behaviors in J-lay on plastic seabed. *J Waterway Port Coast Ocean Eng*. 2012;138(2):77-85.

Wang L, Zhou W, Guo Z, Rui S. Frequency change and accumulated inclination of offshore wind turbine jacket structure with piles in sand under cyclic loadings. *Ocean Eng*. 2020;217:108045.

Xu C, Jiang H, Xu M, Sun D, Rui S. Calculation method for uplift capacity of suction caisson in sand considering different drainage conditions. *Sustainability*. 2023;15(1):454.

Xu P, Du Z, Huang F, Javanmardi A. Numerical simulation of deepwater S-lay and J-lay pipeline using vector form intrinsic finite element method. *Ocean Eng*. 2021;234:109039.

Yang H, Guo Z, Wang L, Qi W. Peak uplift resistance of offshore slender structures shallowly buried in the sloping seabed considering wave actions. *Appl Ocean Res*. 2022;129:103388.

Yang H, Guo Z, Wang L, Dou Y, Liu Z. Experimental study on wave-induced seabed response and force on the pipeline shallowly buried in a submerged sandy slope. *Ocean Eng.* 2022;251:111153.

Yang M, Aubeny CP, Murff JD. Behavior of suction embedded plate anchors during keying process. *J Geotechn Geoenviron Eng.* 2012;138(2):174-183.

Young IR. *Wind-Generated Ocean Waves*. Elsevier; 1999.

Yuan F, Guo Z, Li L, Wang L. Numerical model for pipeline laying during S-lay. *J Offshore Mech Arctic Eng.* 2012;134(2):021703.

Yuan F, Wang L, Guo Z, Shi R. A refined analytical model for landslide or debris flow impact on pipelines. Part I: Surface pipelines. *Appl Ocean Res.* 2012;35:95-104.

Yuan F, Wang L, Guo Z, Xie Y. A refined analytical model for landslide or debris flow impact on pipelines. Part II: Embedded pipelines. *Appl Ocean Res.* 2012;35:105-114.

Zha X, Guo Z, Wang L, Rui S. A simplified model for predicting the accumulated displacement of monopile under horizontal cyclic loadings. *Appl Ocean Res.* 2022;129:103389.

Zhang W, Zhou Z, Pradhan DL, Wang P, Jin H. Design considerations of drag anchors in cohesive soil for floating facilities in the South China Sea. *Mar Struct.* 2022;81:103101.

Zhao C, Kruyt NP, Pouragha M, Wan R. Fabric response to stress probing in granular materials: two-dimensional, anisotropic systems. *Comput Geotech.* 2022;146:104695.

Zhao Y, Liu H. Numerical simulation of drag anchor installation by a large deformation finite element technique. In: *International Conference on Offshore Mechanics and Arctic Engineering* (Vol. 45411, V003T10A011). American Society of Mechanical Engineers. OMAE2014-23476; 2014.

Zhou W, Guo Z, Wang L, Li J, Rui S. Sand-steel interface behaviour under large-displacement and cyclic shear. *Soil Dyn Earthq Eng.* 2020;138:106352.

Zhou W, Guo Z, Wang L, Li J, Rui S. Effect of cyclic jacking on sand-pile interface shear behaviour. *Soil Dyn Earthq Eng.* 2021;141:106479.

Zhou W, Guo Z, Wang L, Li J, Li Y, Rui S. Simplified t-z models for estimating the frequency and inclination of jacket-supported offshore wind turbines. *Comput Geotech.* 2021;132:103959.

Zhou W, Guo Z, Wang L, Zhang Y, Rui S. Numerical model for suction caisson under axial cyclic loadings. *Ocean Eng.* 2021;240:109956.

Zhou W, Wang L, Guo Z, Liu J, Rui S. A novel t-z model to predict the pile responses under axial cyclic loadings. *Comput Geotech.* 2019;112:120-134.

Zhou Z, O'Loughlin CD, White DJ. An effective stress analysis for predicting the evolution of SCR–seabed stiffness accounting for consolidation. *Géotechnique.* 2020;70(5):448-467.

AUTHOR BIOGRAPHIES

Shengjie Rui, Marie Curie fellow. His research topics include mooring line-seabed interaction and trenching, anchor capacity, and interface behavior of marine foundations and soil. He got the PhD at Zhejiang University, and now he is a postdoc in Norwegian Geotechnical Institute (NGI). He was awarded with MSCA Postdoctoral Fellowships 2022. He has published 28 papers and authorized 4 America invention patents, and 15 China invention patents. His Google citation is 216. He was served as Guest Editor in "Frontiers in Marine Science" and "Sustainability" journal.

Kanmin Shen, is a senior engineer and postdoctoral fellow specializing in off-shore geotechnical engineering. His primary focus is on research and technology development for offshore wind structures. He leads several R&D projects funded by organizations such as the National Natural Science Foundation of China and Zhejiang Provincial Natural Science Foundation, as well as several international joint industry projects. Dr. Kanmin Shen has published 27 papers and holds 15 national invention patents. His work has been applied to several global offshore wind farm projects.